Heterogeneous and Homogeneous Diffusivity in an Ion-Conducting Glass

Ranko Richert* and Roland Böhmer
Institut für Physikalische Chemie, Johannes Gutenberg-Universität, 55099 Mainz, Germany
(Received 2 June 1999)

The nature of ion diffusivity in the vitreous conductor $2\mathrm{Ca(NO_3)_2} \cdot 3\mathrm{KNO_3}$ (CKN) was studied by nonresonant dielectric hole burning. Spectral holes in the electric field relaxation are probed subsequent to a high electric sinusoidal burn field. For sufficiently high pump frequencies we are able to induce spectrally selective modifications in the relaxation of the electric modulus, indicating that ionic diffusivity is a spatially varying quantity in glassy CKN. Homogeneous behavior occurs in the regime of low pump frequencies, in which the resistivity approaches its steady state value. Thus, longer-ranged ionic motions lead to a spatial averaging over the heterogeneity of local ion diffusivities.

PACS numbers: 66.30.Hs, 64.70.Pf, 77.22.Gm

The nature of nonexponential relaxation dynamics in supercooled liquids and ionic glass formers is investigated in view of fundamental as well as technological aspects. While above the glass transition temperature, $T > T_g$, the focus is mainly on understanding structural relaxations and their relation to the vitrification process [1]; amorphous ion conductors are also studied below T_g, because of their potential applications in charge storage devices based on solid state ionic materials [2]. Moreover, recent experimental and theoretical efforts have revealed that the relaxation dynamics of noncrystalline materials can be turned into a sensitive diagnostic of their nanoheterogeneity [3–7]. One important consequence of the existence of heterogeneity as regards to dynamical properties is that slow and fast relaxation processes coexist, i.e., the relaxation time is a spatially varying quantity. Recent experiments on various glass formers indeed confirm that it is possible to select slow (or otherwise distinguishable) subensembles [1,8–10]. They also show that these heterogeneities fluctuate in time rather than being of static origin. This means that a selected subensemble becomes dynamically indistinguishable from the ensemble average after some finite reequilibration time.

In all previous selection experiments carried out near but above T_g, the heterogeneity of rotational degrees of freedom has been assessed [1,3,8]. On the other hand, translational motions are of interest when dealing with ionic diffusivity. Numerous concepts were put forward in an attempt to rationalize the ion dynamics in vitreous conductors [11,12], whereas the nature of nonexponential or dispersive electrical responses is yet to be clarified. For these substances, long-ranged ion-ion correlations mediated by Coulomb interactions can be expected to yield an effective averaging over structural inhomogeneities [13]. Moynihan concluded from a kinetic model that such an averaging occurs predominantly in fast ion conductors, characterized by a large decoupling between ionic and structural degrees of freedom [14]. Other well investigated compounds, like the vitreous ion conductor $2\mathrm{Ca(NO_3)_2} \cdot 3\mathrm{KNO_3}$ (CKN), are characterized by an intermediate extent of decoupling [15,16]. For this latter case, Moynihan suggested that the electrical field relaxation should lack an effective averaging and therefore exhibit heterogeneous ion dynamics [14]. This experimental work examines the nature of ion dynamics in CKN, homogeneous versus heterogeneous, thereby addressing one aspect of the above mentioned model. To this end we study the model glass former CKN using nonresonant hole burning (NHB) [8] modified to be directly sensitive to the electrical field relaxation $M(t)$. NHB, a pump and probe method, is based on a frequency selective input of energy provided during a high-voltage burn process. From our measurements carried out below $T_g = 333$ K [17,18] we find that a selection of dynamical subensembles is possible, implying that heterogeneity contributes to the nonexponential character of the ion conduction in CKN. However, this statement holds true only as long as the mean square displacements of the mobile ions do not exceed the length scale of these heterogeneities, which are presumably of structural origin.

Vitreous CKN specimens were prepared as described elsewhere [19]. The 25 μm thick samples were investigated in a spring-loaded, vacuum sealed Invar/sapphire capacitor assembly. For the filled capacitor we determined $\varepsilon_\infty \cdot C_{\mathrm{geo}} = 220$ pF yielding $\varepsilon_\infty \approx 6.5$ in accord with previous results [18]. The voltage $U_c(t)$ across the CKN sample was measured under constant charge conditions for times $10^{-3} < t < 10^2$ s, which then corresponds to the electrical modulus $M(t)/M_\infty$ [19]. $M_\infty = \varepsilon_\infty^{-1}$ denotes the electrical modulus in the high-frequency limit, $t \to 0$. The time dependence of the electrical relaxation as measured at $T = 300$ K is shown in Fig. 1. It can be described using a stretched exponential function,

$$M(t)/M_\infty = A \exp[-(t/\tau)^\beta]. \tag{1}$$

For $T = 300$ K we find $\tau = 1.89$ s, $\beta = 0.79$, and $A = 0.983$ in good agreement with previous measurements [18,19]. The prefactor $A < 1$ accounts for the well-known high-frequency deviations from the stretched exponential pattern [18,19].

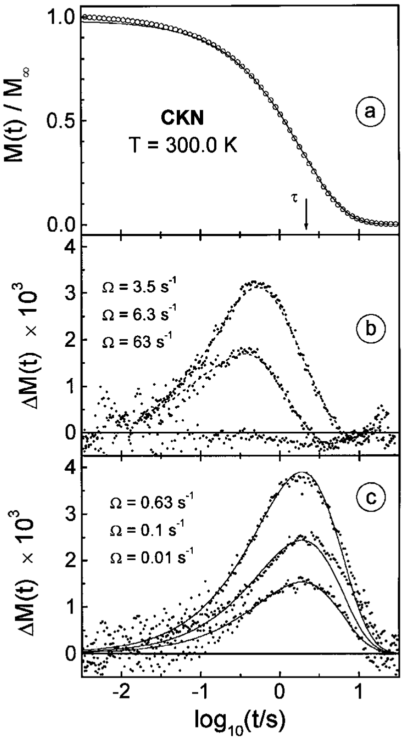

FIG. 1. (a) Time dependent electric field relaxation, $M(t)/M_\infty$, of CKN recorded at $T = 300$ K. Symbols refer to experimental data; the solid line is a stretched exponential fit with $\tau = 1.89$ s and $\beta = 0.79$. Panels (b) and (c) show difference curves $\Delta M(t) = [M(t) - M^*(t)]/M_\infty$ obtained using pump fields of $E_b = 96$ kV/cm and various pump frequencies Ω as indicated in the order from upper to lower curve. The solid lines in (c) correspond to homogeneous modifications, $M_{\mathrm{hom}}(t)$, calculated according to Eq. (4) using $\Delta t = 107$, 67, and 42 mK.

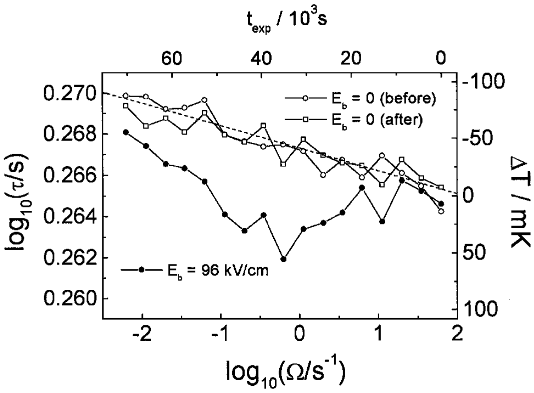

FIG. 2. Closed symbols: Time constants τ^* at which the response $M^*(t)$, modified by pumping with $E_b = 96$ kV/cm, has decayed to M_∞/e as a function of pump frequency Ω. Open symbols: Time constants τ from the equilibrium responses, recorded before (○) and after (□); the pump sequence agrees within experimental error. Measurements appearing on the right-hand side of the diagram were taken first. The top axis shows how much later subsequent data were taken.

Application of one cycle of a sinusoidal burn voltage, $U_b \sin(\Omega t)$ yields modified response functions, $M^*(t)/M_\infty$, using the following technique. Subsequent to the burn cycle and a waiting period, $t_w = 10^{-3}$ s, the capacitor was charged to a small voltage $[|U_c(0)| = 4$ V$]$ and immediately (≤ 400 μs) insulated from the source by a high-impedance relay. This procedure creates a step in the dielectric displacement which, due to the high resistance (10^{15} Ω) of the detection circuit, remains essentially constant during the detection time. For the measurements of M^* we used the phase cycle described previously [8].

At a sample temperature of $T = 300$ K (constant within ±5 mK for about 10^6 s) we carried out NHB experiments at 14 pump frequencies, $6.3 \times 10^{-3} \leq \Omega \leq 63$ s^{-1} and five different burn voltages, $100 \leq U_b \leq 240$ V, equivalent to burn fields $40 \leq E_b \leq 96$ kV/cm. Between the measurements the sample was kept under zero field for periods of 10^3 s ($\gg \tau$) in order to allow for a complete reequilibration. In Fig. 2 we show time constants τ [from $M(t)$] and τ^* [from $M^*(t)$] collected in the course of about 7×10^4 s. Three features are observed in this plot. (i) Pumping decreases the modulus relaxation time, $\tau^* < \tau$, to an extent which depends on Ω. The maximum hole burning effects (near $\Omega = 0.5$ s^{-1}) are only 0.005 decades and thus very small. (ii) The values of $\log_{10}(\tau/\mathrm{s})$ measured before and after the pump cycle coincide within 8.5×10^{-4}, indicating that hole burning does not lead to irreversible changes in the relaxation behavior. (iii) The equilibrium relaxation times τ show a systematic increase. This latter effect can be assigned to physical aging by noting that subsequent to cooling down the freshly prepared sample and stabilizing it at 300 K for 134 h, the measurements at the highest Ω were taken first. The approximate time increments t_{exp} at which later data have been acquired can be read off from the top axis of Fig. 2.

A detailed view of the changes induced by the pump process is shown in Figs. 1(b) and 1(c) as the difference between equilibrium and modified responses,

$$\Delta M(t) = [M(t) - M^*(t)]/M_\infty . \qquad (2)$$

Pumping at a sufficiently large frequency [cf. the $\Omega = 63$ s^{-1} curve in Fig. 1(b)] does not alter the relaxation function. A decrease of Ω leads to difference spectra, $\Delta M(t)$, which are characterized by an increase of both their peak amplitude, ΔM_m, and their peak position, t_m. The fact that pumping at frequencies in excess of $\Omega_c = 3$ s^{-1} [Fig. 1(b)] results in Ω dependent positions of the "holes" $\Delta M(t)$ implies a frequency selective modification of the conductivity response. This constitutes a clear indication of heterogeneous ion dynamics, such that a spatial distribution of diffusivities has to be involved in the nonexponential nature of the electrical behavior [8,20]. However, for $\Omega \leq \Omega_c$ [Fig. 1(c)] the situation changes: Here, ΔM_m decreases with Ω and t_m remains close to the time constant, τ, of the equilibrium $M(t)$

curve. An even better impression of the existence of two different regimes can be gained from Fig. 3, in which we plot ΔM_m as well as t_m as a function of Ω.

The $t_m(\Omega)$ results of Fig. 3(a), obtained for various pump fields E_b, demonstrate the good reproducibility of the measured effects. For $\Omega \geq \Omega_c$ we find $t_m \propto \Omega^{-\alpha}$ with $\alpha = 0.5 \pm 0.1$. NHB experiments on other materials have shown that $\alpha \approx 1$ is characteristic of practically flat relaxation time distributions [20]. The exponent α observed for CKN is much smaller, consistent with the narrower distribution as characterized by $\beta = 0.79$. As in previous studies [8,20] the hole depth, ΔM_m, varies as E_b^2. More importantly, Fig. 3(b) reveals that in the heterogeneous regime ΔM_m is proportional to the dielectric loss ε'' of CKN [18]. This means that for high enough frequencies ($\Omega \geq \Omega_c$), the depths of the holes are linear in the absorbed energy $Q \propto \varepsilon''(\Omega) E_b^2$.

Without going into further details, we note that the holes burned in the frequency range $0.02 \leq \Omega \leq 3.5\ \mathrm{s}^{-1}$ refill with a time constant of $1/\Omega$. By varying the waiting time, t_w, between burn cycle and detection, this fading has been measured in terms of ΔM_m with the result of $\Delta M_m(t_w) \propto \exp(-\Omega t_w)$. The concomitant peak positions, t_m, do not change significantly as a function of t_w.

In order to see why the behavior of $\Delta M(t)$ changes near Ω_c, it is instructive to compare in Fig. 3(a) $t_m(\Omega)$ with the resistivity $\rho(t)$ [19] of CKN,

$$\rho(t) = \frac{1}{\varepsilon_0} \int_0^t M(t')\, dt'. \tag{3}$$

Near the time given by $1/\Omega_c$, it is seen that $\rho(t)$ changes from dispersive short-time behavior to steady state Ohmic transport. The interpretation which is suggested by this coincidence is that for low Ω, i.e., for long enough times, the ions have traveled a sufficient distance along their conductivity pathway in order to allow for an effective spatial averaging over a representative set of local environments. On this long time scale, selective modifications are impossible and the dynamics are bound to appear homogeneous rather than heterogeneous. In this homogeneous regime, $\Omega \leq \Omega_c$, the modified response $M^*(t)$ is expected to be shifted uniformly along the logarithmic time axis with $\tau^* < \tau$, analogous to a slight increase in an effective temperature [8]. Thus, in order for our interpretation to be valid for $\Omega \leq \Omega_c$, the difference signal, $\Delta M(t)$, should be proportional to the derivative, $\partial M(t)/\partial \log_{10}(t/\mathrm{s})$. This derivative displays a (Ω invariant) peak at times at which $M(t)$ has decayed to $1/e$ of its initial value M_∞, thus explaining the observation of a constant t_m made in Fig. 3 for $\Omega \leq \Omega_c$. The solid lines in Fig. 1(c) represent such derivative curves, $\Delta M_{\mathrm{hom}}(t)$, and are seen to be in excellent agreement with our data.

For a more quantitative analysis of $\Delta M(t)$ at $\Omega \leq \Omega_c$ we note that the conductivity relaxation time of CKN in its glassy state obeys the Arrhenius law, $\tau = \tau_0 \exp(B/T)$, here with $B = 4980$ K. Use of $\partial \log_{10}(\tau/\mathrm{s})/\partial T = -B/T^2$ allows one to transform a change in relaxation time to an effective temperature change, as done in Fig. 2. Along these lines, a certain ΔT translates into a predicted "homogeneous" difference signal,

$$\Delta M_{\mathrm{hom}}(t) = -\frac{B \cdot \Delta T}{T^2} \frac{\partial M(t,T)/M_\infty}{\partial \log_{10}(t/\mathrm{s})}. \tag{4}$$

Since our experiments are conducted under isothermal conditions, the coefficient ΔT refers to a shift in "fictive" or "structural" temperature [21]. The lines in Fig. 1(c) are fits using Eq. (4) with ΔT as the adjustable parameter. The maximum ΔT that we find is about 100 mK, observed for $E_b = 96$ kV/cm and $\Omega = 0.63\ \mathrm{s}^{-1}$. The energy per volume absorbed in one pump cycle is given by $Q = \pi \varepsilon_0 \varepsilon''(\Omega) E_b^2$, which in our case is $Q \approx 3\ \mathrm{mJ/cm^3}$. This yields a shift $\Delta T = Q/\Delta c_p$ of the effective temperature if the specific heat capacity, Δc_p, associated with the excitation of the mobile ions is known. This heat capacity can be expected to be smaller than the step ΔC_p associated with the structural relaxation appearing in the glass transformation range. With $\Delta C_p = 1.2\ \mathrm{J/(K\,cm^3)}$ for CKN near T_g [17], it turns out that the observed $\Delta T \approx 100$ mK is compatible with a ratio $\Delta c_p/\Delta C_p$ of order 10^{-2}. Although the relevant heat capacity contribution Δc_p has not yet been determined for CKN,

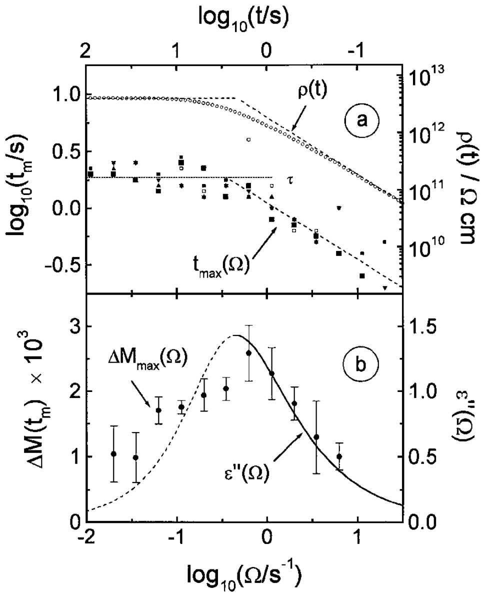

FIG. 3. (a) Solid symbols reflect experimental results for the peak position, t_m, of $\Delta M(t)$ as a function of $\log_{10}(\Omega/\mathrm{s}^{-1})$ for various pump fields, $40 \leq E_b \leq 96$ kV/cm. The dashed line represents a power law $t_m \propto \Omega^{-0.5}$, the horizontal line indicates $t_m = \tau = 1.89$ s. The open symbols show the time dependent resistivity $\rho(t)$ as calculated from the $M(t)$ data. (b) Experimental results for the peak amplitudes, $\Delta M_m \equiv \Delta M(t_m)$, as a function of $\log_{10}(\Omega/\mathrm{s}^{-1})$ for $E_b \leq 80$ kV/cm. The ε'' curve outlines the dispersive component of the dielectric loss [18], whose high-frequency wing shows good agreement with the Ω dependence of the amplitude ΔM_m.

$\Delta c_p \ll \Delta C_p$ has similarly been found for several other ion-conducting glasses [22].

In recent years, dynamic heterogeneity has been recognized as the dominant origin of nonexponential orientational correlation functions in supercooled liquids, where the local time constants are assumed to fluctuate on the time scale of the structural relaxation. From our NHB results on glassy CKN for $\Omega \geq \Omega_c$, we conclude that translational ion motion is also subject to heterogeneities. In this case spatial variations associated with the structure can safely be assumed static, because at $T = 300$ K the relaxation time of the CKN structure is orders of magnitude longer than that of its electrical response. The present experimental evidence of heterogeneous electrical relaxation is consistent with a recent prediction concerning intermediately decoupled ion conductors like CKN [14]. However, a more complete assessment of the underlying model [14] requires analogous experiments on fast or highly decoupled ionic conductors (like $NaO_2 \cdot 3SiO_2$) in order to confirm or contradict the existence of a correlation between the decoupling ratio and the degree of heterogeneity.

To summarize, we were able to induce spectral holes in the conductivity response of the glassy ionic conductor CKN, demonstrating that spectrally selective techniques, which previously have been used only to study rotational motions, can be applied successfully to the investigation of translational degrees of freedom, as well. More importantly, our results from nonresonant hole burning provide evidence that a spatial distribution of diffusivities governs the dispersive regime of conductivity relaxation. Spatial averaging over the local electrical relaxations is observed via a crossover from the heterogeneous to the homogeneous regime at a frequency Ω_c which coincides with that characterizing the transition from dispersive (ac) to steady state (dc) conductivity (or likewise resistivity). Because the mean square displacement of the ions is a function of the burn frequency Ω, the value of Ω_c indicates where the average ion displacement has reached the characteristic length scale of the heterogeneities seen at $\Omega \geq \Omega_c$. Referring to the observations in the low-frequency range, it is also gratifying to note that the NHB technique is found capable of identifying dynamic homogeneity and quantifying the subtle changes in fictive temperature induced by the burn process.

We thank H. Wagner for the preparation of the CKN samples. Financial support by the Fonds de Chemischen Industrie is gratefully acknowledged.

*Permanent address: Department of Chemistry and Biochemistry, Arizona State University, Tempe, AZ 85287-1604.

[1] K. Schmidt-Rohr and H.W. Spiess, Phys. Rev. Lett. **66**, 3020 (1991).

[2] C.A. Angell, C. Liu, and E. Sanchez, Nature (London) **362**, 137 (1993).

[3] U. Tracht, M. Wilhelm, A. Heuer, H. Feng, K. Schmidt-Rohr, and H.W. Spiess, Phys. Rev. Lett. **81**, 2727 (1998).

[4] E. Vidal Russell, N.E. Israeloff, L.E. Walther, and H. Alvarez Gomariz, Phys. Rev. Lett. **81**, 1461 (1998).

[5] R. Richert, J. Phys. Chem. B **101**, 6323 (1997); R. Richert and M. Richert, Phys. Rev. E **58**, 779 (1998).

[6] C. Bennemann, C. Donati, J. Baschnagel, and S.C. Glotzer, Nature (London) **399**, 246 (1999).

[7] P.H. Poole, Curr. Opin. Solid State Mater. Sci. **3**, 391 (1998); H. Sillescu, J. Non-Cryst. Solids **243**, 81 (1999).

[8] B. Schiener, R.V. Chamberlin, G. Diezemann, and R. Böhmer, J. Chem. Phys. **107**, 7746 (1997).

[9] S. Sen and J.F. Stebbins, Phys. Rev. Lett. **78**, 3495 (1997).

[10] M.T. Cicerone and M.D. Ediger, J. Chem. Phys. **103**, 5684 (1995).

[11] Solid State Ion. **105**, 1–302 (1998), edited by A. Bunde, K. Funke, and M.D. Ingram.

[12] K.L. Ngai, J. Non-Cryst. Solids **203**, 232 (1996); D.L. Sidebottom, Phys. Rev. Lett. **82**, 3653 (1999).

[13] K.L. Ngai and S.W. Martin, Phys. Rev. B **40**, 10 550 (1989).

[14] C.T. Moynihan, J. Non-Cryst. Solids **235–237**, 781 (1998).

[15] C.A. Angell, Chem. Rev. **90**, 523 (1990).

[16] F. Mezei, W. Knaak, and B. Farago, Phys. Rev. Lett. **58**, 571 (1987); P. Lunkenheimer, A. Pimenov, and A. Loidl, Phys. Rev. Lett. **78**, 2995 (1997).

[17] C.T. Moynihan, H. Sasabe, and J.C. Tucker, in *Proceedings of the International Symposium on Molten Salts*, edited by J.P. Pennsler, J. Bronstein, D.R. Morris, K. Nobe, and W.P. Richards (Electrochemical Society, Pennington, NJ, 1976), p. 182.

[18] F.S. Howell, R.A. Bose, P.B. Macedo, and C.T. Moynihan, J. Phys. Chem. **78**, 631 (1974); A. Pimenov *et al.*, J. Non-Cryst. Solids **220**, 93 (1997).

[19] H. Wagner and R. Richert, J. Appl. Phys. **85**, 1750 (1999).

[20] O. Kircher, B. Schiener, and R. Böhmer, Phys. Rev. Lett. **81**, 4520 (1998).

[21] J. Baschnagel, K. Binder, and H.P. Wittmann, J. Phys. C **5**, 1597 (1993); C.T. Moynihan, Solid State Ion. **105**, 175 (1998).

[22] M. Hanaya, M. Nakayama, A. Hatate, and M. Oguni, Phys. Rev. B **52**, 3234 (1995); M. Hanaya, M. Nakayama, and M. Oguni, J. Non-Cryst. Solids **172–174**, 608 (1994).